IOSR Journal of Engineering (IOSRJEN) **www.iosrjen.org**
ISSN (e): 2250-3021, ISSN (p): 2278-8719
Vol. 06, Issue 10 (October. 2016), ||V2|| PP 07-17

Conformational study of different surfactants in bentonite and PET nanocomposites

Itamara F. Leite[1*], Suédina M. L. Silva[2], Marcus V. P. Santos[3], Oscar M. L. Malta[3], Ricardo L. Longo[3]

[1]*Departamento de Engenharia de Materiais, Universidade Federal da Paraíba, Cidade Universitária, João Pessoa - PB, 58051-900, Brazil,*
[2]*Unidade Acadêmica de Engenharia de Materiais, Universidade Federal de Campina Grande, Rua Aprigio Veloso, 882, Bairro Universitário, Campina Grande, PB, 58429-140, Brazil,*
[3]*Departamento de Química Fundamental, Universidade Federal de Pernambuco, Av. Prof. Luiz Freire, s/n, Cidade Universitária, Recife, PE, 50740-540, Brazil,*

Abstract: - The interlayer swelling and molecular packing of the organic salts in organoclays is important to the formation and design of polymer nanocomposites. The sodium bentonite clay (AN) were modified by the MA, $(C_{16}H_{33}N(CH_3)_3)^+$, and BP, $(C_{16}H_{33}P(C_4H_9)_3)^+$ cations yielding the organoclays ANOMA and ANOBP. Infrared spectroscopy, thermal analysis and X-ray diffraction characterization of the modified clays showed that the BP cation induces a larger basal interlayer separation than MA. However, nanocomposite with an intercalated morphology was observed for the poly(ethylene terephthalate) PET/ANOMA hybrid. Conformational Monte Carlo searches based on AM1 (Austin Model 1) and molecular mechanics (MMFF94) methods were performed for the organic MA and BP cations as well as for MP $(C_{16}H_{33}P(CH_3)_3)^+$, and BA, $(C_{16}H_{33}N(C_4H_9)_3)^+$. MA and BA cations presented a predominant linear or extended (*anti*) conformation, whereas BP and BA have significant contributions from folded conformations. These molecular modeling results explained the observed spectroscopic, thermal and structural properties of the modified ANOMA and ANOBP clays as well as those of PET/ANOMA and PET/ANOBP hybrids. In addition, a new intercalation model considering these folded conformations was proposed.

***Keywords*: -** *organoclays; folded and extended conformations; intercalation; nanocomposites*

I. INTRODUCTION

The study of nanocomposites has attracted extensive industrial and academic attention during the last decade. Clays are widely used in nanocomposite formation because of their special nanoscale layered structures and their low costs. However, to insert mostly hydrophobic polymer chains into the hydrophilic silicate layers, cationic surfactants, such as alkylammonium or alkylphosphonium salts, are usually used to modify the surface properties of the clays prior to mixing with polymers [1-3]. The combination of the hydrophobic nature of the surfactant and the layered structure of the silicate clays leads to unique physicochemical properties. The organically modified clays have been referred to as *organoclays* or *organophilic-clay*s and are widely used as nanocomposite precursors [4-5]. In industries, organoclays are also used as adsorbents for organic pollutants [6], rheological control agents [7] and electric materials [8]. In these applications, the behavior and properties of the organoclays strongly depend on the structure and the molecular environment of the organic molecules within the galleries [9].

A large variety of organoclays have been synthesized using different surfactants [10-15] and their structures have been characterized using various techniques, including Fourier transform infrared spectroscopy (FTIR) [16-18], X-ray diffraction (XRD) [11-12], thermogravimetric measurement (TG) [19-22], magic angle spinning nuclear magnetic resonance (MAS NMR) [23-24] and transmission electron microscopy (TEM) [25-26]. These techniques can yield detailed information about the interlayer structure; conformations of the intercalated surfactant, and the thermal stability of the resulting organoclays.

Capkova et al. [27] studied the dependence of the basal spacing as a function of different ammonium salts using classical molecular dynamics simulations. Using the same method, Hackett et al. [28] analyzed the distribution of the methyl groups of the alkyl chains of alkylammonium salts confined between two clay layers. Tanaka and Goettler [29] investigated the influence of different alkylammonium salts and amino acids on the interaction energy between organoclay and polyamide 6×6 matrices. Balasz et al. [30] created mesoscopic models to study the effects of the surfactant on the exfoliation. However, to our knowledge, there are no studies about the effects of folding degree of the large alkyl chain $CH_3(CH_2)_{15}$ as well as the smaller alkyl substituents (methyl × butyl) of the surfactants on the basal spacing of modified clays.

As a result, the main goal of this work is to establish relationships between the chemical structure of the surfactants and the increase of the basal spacing in modified clays. The chemical structures of the alkylammonium and alkylphosphonium salts were quantified by their molecular volume, their steric hindrance and their folding degree. These quantities were calculated with force fields (MMFF94) and quantum chemical methods (AM1) using a Monte Carlo approach for conformational searches. These calculated quantities were correlated with experimental data obtained with FTIR, XRD and TG techniques applied to modified bentonite clays.

II. EXPERIMENTAL

2.1. Materials

Sodium bentonite clay, Argel 35 (AN) was supplied by Bentonit União Nordeste (BUN-Campina Grande/Brazil), in powdered form, with particle sizes smaller than 45 μm. The cation exchange capacity (CEC) of this bentonite was determined by method described by Phelps and Harris [31] and found to be 92 meq/100 g. The most important clay mineral present in the Argel 35 bentonite is a sodium montmorillonite (around 63%) as determined by XRD-6000 software. There is also a minor fraction of non-layered minerals such as quartz, kaolinite and carbonates [32-33]. The surfactants, cetyl trimethyl ammonium bromide (MA), $(C_{16}H_{33}N(CH_3)_3)^+Br^-$, and hexadecyl tributyl phosphonium bromide (BP), $(C_{16}H_{33}P(C_4H_9)_3)^+Br^-$, were used without further purification to modify the bentonite clay (AN). These surfactants were supplied by Vetec and Sigma-Aldrich, respectively.

Poly(ethylene terephthalate) (PET), BG1180-W, was obtained from Braskem/BA as white pellets and was used as the polymeric matrix for the preparation of nanocomposites. This polymer has a large intrinsic viscosity 0.80 ± 0.02 dl/g; an acetaldehyde contamination of 1.0ppm; 245 ± 5ºC melting point and a density range 1.39 – 1.41 g/cm^3.

2.2. Organic modification of bentonites

The pristine AN bentonite was organically modified by ion-exchange reaction with the cetyl trimethyl ammonium bromide (MA), $(C_{16}H_{33}N(CH_3)_3)^+Br^-$, and hexadecyl tributyl phosphonium bromide (BP), $(C_{16}H_{33}P(C_4H_9)_3)^+Br^-$, surfactants following a previously described procedure [32]. These salts were slowly added to aqueous bentonite dispersions (2% w/v), under vigorous stirring at 70 ± 5ºC in amounts corresponding to 100% of the clay's theoretical ion exchange capacity (92 meq/100 g). After 30 min under stirring, the clay was keep standing at room temperature for 24h. Afterwards, the sample was filtered and washed free of bromide anions, dried at 60ºC for 48h and grounded in an agate mortar to pass through 325 mesh sieve. The AN bentonite organically modified with the MA and BP surfactants was coded ANOMA and ANOBP, respectively. Pristine and modified bentonites were characterized by Fourier transform infrared spectroscopy (FTIR), X-ray diffraction (XRD) and thermogravimetric analysis (TG).

2.3. PET nanocomposites preparation

PET/organoclay nanocomposites with a nominal content of 1 wt% organoclay were melt compounded in a Haake torque rheometer operating at 260ºC and 60 rpm for 10 min and denoted as PET/ANOMA and PET/ANOBP. Prior to processing the PET and the modified clays were dried for 6h at 160ºC and 60ºC, respectively. Immediately after processing hybrids for XRD characterization were compression molded (2 min under compression) as disc shaped specimens with 25 mm diameter and 1 mm of thickness in a hot press operating at 260ºC.

2.4. Characterization

Infrared spectroscopy (FTIR) analyses of the clays were performed in Nicolet Avatar TM on KBr pressed disks. For each sample, 0.07 mg KBr and 0.05 mg bentonite were weighted and then were ground in an agate mortar before making the pellets. Spectra were taken with a 2 cm^{-1} resolution in a wavenumber range from 4000 to 400 cm^{-1} with 20 scans.

X-ray diffraction (XRD) experiments of clays and PET hybrids were performed in a Shimadzu XRD-6000 diffractometer using the CuKα radiation (λ = 1.5406 Å), operating at 40 kV and 30 mA with 2θ varying from 1.5° to 10º. XRD plots were used to determine the mean interlayer spacing of the basal plane (d_{001}) of pristine and organophilic clays and in the PET hybrids.

Thermogravimetric analyses (TG) were performed using a Shimadzu thermal analyzer, TG S1HA. Approximately 15 mg of sample was heated in a platinum crucible, from room temperature to 1000ºC at a heating rate 10ºC/min under air atmosphere at 50 mL/min.

2.5. Molecular modeling

Conformational searches for the organic salts were performed with Monte Carlo method using 5000 K temperature to ensure a proper sampling of the conformational space. The energies were computed with quantum chemical, AM1 [34-35], and force field, MMFF94 [36], methods. A large list of the most stable conformers was kept, but only those whose Boltzmann weight at room temperature added to 0.95 were used in

the analyses. Each one of these conformers had their structures optimized using the same method used in the conformational search. In addition to the (relative) energies, other properties have been computed, namely, molecular volume (from electron density and van der Waals radii) and degree of folding of the large alkyl chain. This latter property was calculated from the geometrical parameters (large and small axes) of an ellipsoidal cavity that contains the salt species.

In addition to the MA, $(C_{16}H_{33}N(CH_3)_3)^+$, and BP, $(C_{16}H_{33}P(C_4H_9)_3)^+$, cations used in the experiments, the BA, $(C_{16}H_{33}N(C_4H_9)_3)^+$, and MP, $(C_{16}H_{33}P(CH_3)_3)^+$, cations were also employed in the molecular modeling studies for comparison and prediction purposes.

III. RESULTS AND DISCUSSIONS

The FTIR spectra of the organic salts MA and BP and their respective modified clays (ANOMA and ANOBP) are presented in Fig. 1. It can clearly be observed that the salts have been intercalated into the clays due to the presence of vibrational bands in the 2921 – 2850 cm^{-1} region assigned to asymmetric (ν_{as}) and symmetric (ν_s) stretches of CH_2 groups as well as band in the 1478 – 1449 cm^{-1} region assigned to asymmetric angular deformations (δ_{as}) of CH_2 and CH_3 groups in the ANOMA and ANOBP samples matching the spectra of the isolated salts. These results are corroborated by similar studies and analyses available in the literature [37-41].

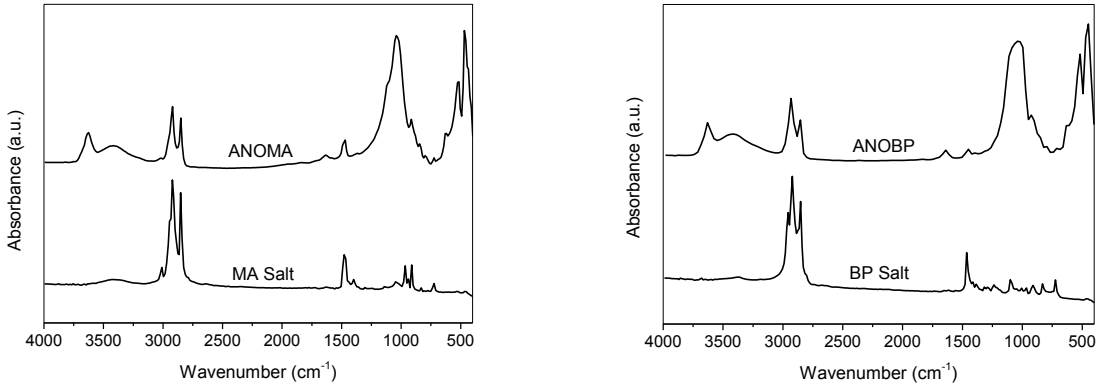

Fig. 1 FTIR spectra of the MA salt and ANOMA modified clay (left) and the BP salt with the ANOBP modified clay

It should also be noted from Fig. 1, and more clearly from Fig. 2 and Table 1, that the asymmetric (ν_{as}) stretch of CH_2 groups has a distinct behavior for the MA and BP salts. Namely, there are practically no changes in this band when the MA salt is intercalated in the clay. This indicates that the alkyl chains of the surfactant confined into the clay galleries adopt an essentially *anti* conformation [42]. Note that this conformation has also been improperly denominated as *trans*. Whereas for the BP modified clay (ANOBP) this asymmetric (ν_{as}) stretch is blue shifted (~10 cm^{-1}) indicating that the *gauche* conformation of the alkyl chain is preferred [42-43]. Note also that the symmetric (ν_s) stretches of CH_2 groups are quite insensitive to the intercalation of the organic salt, thus showing that the asymmetric (ν_{as}) stretches of CH_2 groups are an interesting probe for the intercalation and the conformation of surfactants.

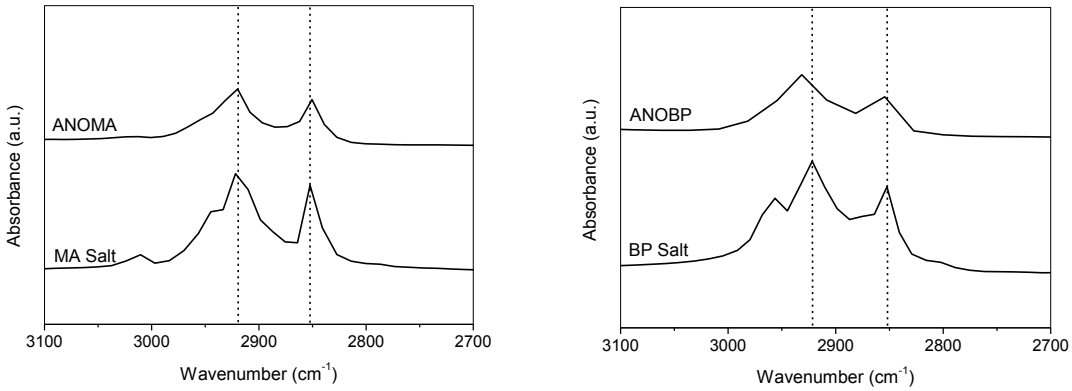

Fig. 2 FTIR spectra in the 2700-3100 cm^{-1} region comparing the isolated MA (left) and BP(right) salts and modified clays ANOMA (left) and ANOBP (right)

FTIR spectra can still yield more important information on composition and structure of clays. The FTIR spectrum of pristine AN clay illustrated in Fig. 3 presents a band at 3626 cm^{-1} assigned to the O-H stretching frequencies of the clay's own hydroxyl groups [44-45]. In the regions near 3450 and 1640 cm^{-1} there are also O-H stretching and angular deformation modes assigned to the adsorbed water molecules [38, 40], respectively. At lower wavenumbers the vibrations associated with Si-O are observed around 1030 cm^{-1} and as well as the ones related to the octahedral aluminosilicate layers at 905 and 472 cm^{-1} [46-47]. It is noticeable that the positions and shapes of these bands are practically unchanged with the modification by the organic salts.

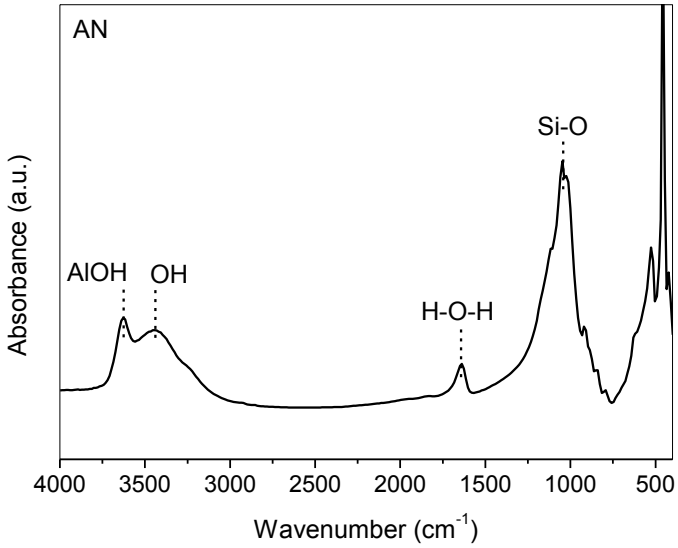

Fig. 3 FTIR spectrum of pristine sodium bentonite clay

Table 1 Wavenumber and assignment of selected bands of FTIR spectra of surfactants (organic salts), pristine bentonite and organically modified bentonite

Sample	ν(OH)	ν(OH) H_2O	δ(HOH)	$\nu_{as}(CH_2)$; $\nu_s(CH_2)$	δ_{as}(C-H)	ν(Si-O)	Si-O-Al
AN	3626	3452	1646	—	—	1036	905-472
MA Salt	—	—	—	2921; 2851	1478	—	—
ANOMA	3629	3415	1633	2919; 2850	1472	1040	908-466
BP Salt	—	—	—	2921; 2852	1468	—	—
ANOBP	3629	3421	1640	2931; 2854	1449	1042	916-464

ν - stretching; ν_{as} - asymmetric stretch; ν_s - symmetric stretch; δ - angular deformation and δ_{as} - asymmetric angular deformation

The pristine bentonite and organically modified bentonites were also characterized by X-ray diffraction (XRD) techniques and their diffraction patterns are shown in Fig. 4. From these difractrograms it is possible to determine that interlayer basal distances (d_{001}) increased 43% and 71% in the modified ANOMA and ANOBP clays, respectively, when compared to the unmodified AN. These data corroborate the FTIR results that the organic cations are intercalated in the basal spacing, thus yielding organophilic clays [37, 48]. A likely explanation for the larger d_{001} distance induced by the BP compared to the MA salt is due to its larger ionic head containing tributyl phosphonium group, $(-P(C_4H_9)_3)^+$, compared to the trimethyl ammonium, $(-N(CH_3)_3)^+$, one. Indeed, there are reports in the literature that the increase of interlayer distance in clay minerals [49], smectite and synthetic micas [50] depend upon the size of the alkyl chains, the packing and the conformation of the surfactant molecule within the clay galleries. Also, it has been proposed [52] that hexadecyl tributyl phosphonium (BP) bromide salt covers efficiently clay surfaces, which decreases the interlayer interactions, thus increasing the basal spacing.

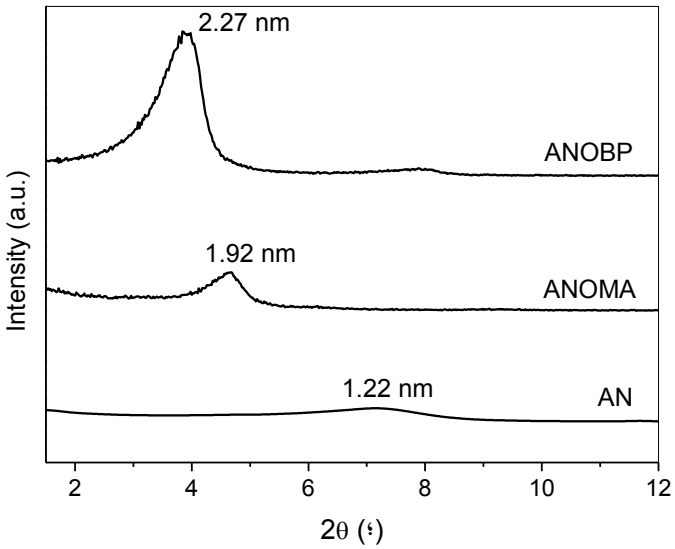

Fig. 4 XRD difractrograms of unmodified (AN) and organically modified clays (ANOMA and ANOBP) with MA e BP salts. The numbers are the interlayer basal distances (d_{001})

Similarly, the thermogravimetric (TG) curves for AN, ANOMA and ANOBP are presented in Fig. 5. From these curves it was possible to estimate for pristine bentonite a 6.67% (at 74°C) water loss and 3% (~700°C) dehydroxylation of the aluminosilicate surface [53]. The organically modified clays showed a distinct thermal behavior with four regions readily identifiable: (I) water loss between 40 and 150ºC; (II) organic substrates between 150 and 550ºC; (III) dehydroxylation of the montmorillonite 550 and 700ºC; and, probably, (IV) carbon residue losses above 700ºC [53-54]. More quantitatively, from Fig. 5 and Table 2 it is clear that the water contents in the modified clays are smaller than that in unmodified clay, indicating that the hydrophilic activity of bentonite is greatly reduced upon organic modification. There are at least two reasons for the decrease of water contents in organoclays [38]: the large organic cations exclude water molecules from the interlayer spaces and the much smaller hydration enthalpies of large organic cations compared to alkaline metal ions. The latter reasoning also explains the much lower temperatures (~50°C) for water losses in organoclays, since the large organic cation weakens the water-clay interactions, in addition to the much weaker water-quaternary cations interaction. The mass loss due to surfactant degradation is larger for ANOMA than ANOBP. This is due to the larger thermo-stability of the BP salt towards oxidation compared to the MA salt according the data presented Table 2. These results corroborate the observed thermal behavior of modified clays, where the nature of the quaternary cation (alkyl chain length, number of alkyl chains and heteroatom) is determinant of the thermal stability [21, 51, 53, 55]. According, alkyl phosphonium salts are more suitable for modifying clays that need to be submitted to high temperature treatments. In addition to the intrinsic thermal stability of the organic salt towards oxidation, the aluminosilicate surface being basic can induce the degradation of the surfactants via chemical reactions such as Hoffmann elimination and nucleophilic attacks within the clay galleries [55]. These processes might explain the reasons that the modified ANOMA and ANOBP clays have decomposition temperatures lower than those of the respective MA and BP pure salts, as presented in Table 2.

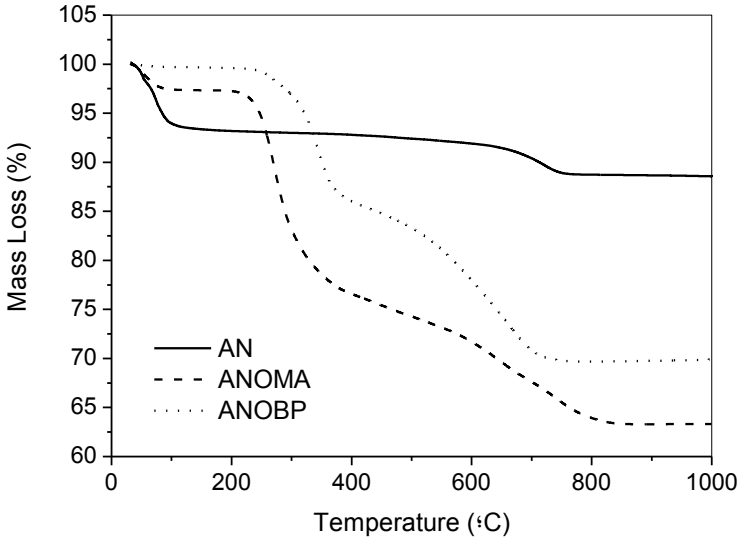

Fig. 5 Thermogravimetric (TG) curves for unmodified (AN) and organically modified clays (ANOMA and ANOBP) with MA e BP salts

Table 2 Temperatures (ºC) at mass losses (%) for pristine AN bentonite clay, surfactants and organoclays, and relative amount of incorporated salts into modified clays

Samples	Water loss		Surfactant loss		Dehydroxylation		Surfactant incorporated
	T_{Dmax}	(%)	T_{Dmax}	(%)	T_{OH}	(%)	(%)
AN	74.0	6.67	—	—	720.0	3.63	—
MA Salt	—	—	283.1	93.65	519.3	5.80	—
ANOMA	54.0	2.66	272.8	20.86	688.9	13.12	98.8
BP Salt	—	—	393.2	98.47	—	—	—
ANOBP	46.0	0.69	342.7	13.98	665.0	15.14	41.0

T_{Dmax}: temperature at the maximum decomposition

The XRD difractrograms for the PET/organoclay hybrids containing 1% mass of clay are presented in Fig. 6. It can be observed that the basal distance (d_{001}) in the PET/ANOMA hybrid is larger than that in the modified ANOMA clay, whereas this distance remains practically unchanged in the PET/ANOBP hybrid compared to the ANOBP. It can thus be inferred that nanocomposite with an intercalated morphology has been obtained only for the organoclay ANOMA, despite the fact that the modified ANOBP clay has a larger basal distance (d_{001}). This might be due to the distinct conformations of the MA and BP cations within the clay galleries as well as different affinities between the PET terminal groups and the organic cations. Indeed, it has been proposed that the success for exfoliation of nanocomposites into layer is associated with the presence of strong interactions between the clay and the polymer [56-58]. Thus, the affinity polymer-clay is essential for a proper dispersion of the polymer load and thus favoring the nanocomposite formation with intercalated and/or exfoliated morphologies.

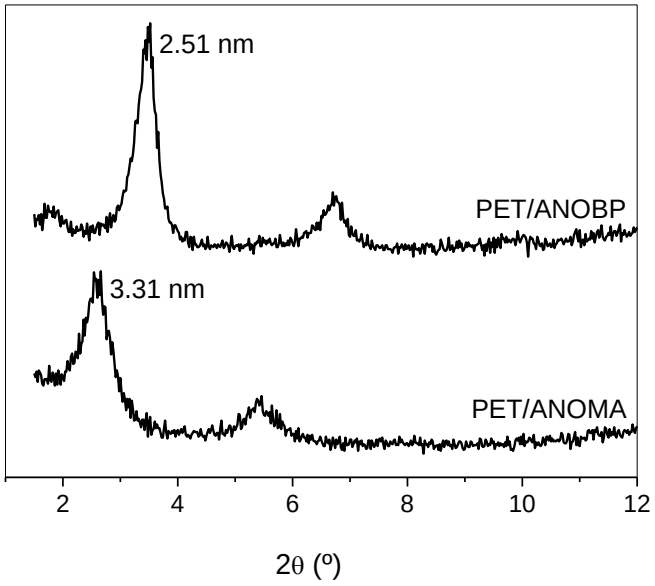

Fig. 6 XRD difractrograms of PET/organoclay hybrids containing 1% mass of modified ANOMA and ANOBP clays. The numbers are the interlayer basal distances (d_{001})

The molecular modeling of the organic cations can provide some explanations for the distinct behavior of the MA and BP on the clay modification as well as the differences in formation of PET/organoclay hybrids. For the MA cation the lowest energy 14 conformers are needed to yield 95.2% of the total Boltzmann distribution and two most stable, that adds up to 80.5%, are illustrated in Fig. 7a. A similar behavior has been found for the MP cation where also 7 conformers were needed to yield at least 95.2% of thermal distribution and the two most stable ones are responsible for 85%. These results indicate that the linear or extended (*anti*) conformation of the large alkyl chain is independent of the nature of the heteroatom, which corroborate the FTIR interpretation that the wavenumbers of asymmetric stretches of CH_2 groups remains unchanged in the MA cations due to its *anti* conformation either isolated or in the organoclay.

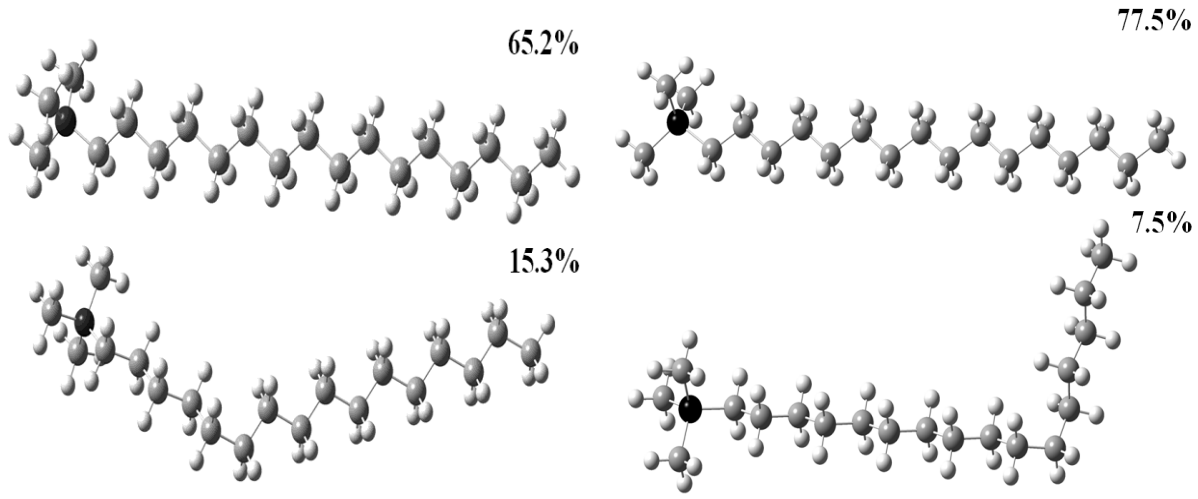

Fig. 7 Most stable conformers of MA (a) and MP (b) cations. The numbers refer to the conformer weight in the thermal distribution. These are the results of a Monte Carlo conformational search using the MMFF94 force field

Similar analyses have been performed for the BA and BP cation. For the BA cation the 9 lowest energy conformers have a 95.9% contribution to thermal distribution and the most relevant ones are illustrated in Fig. 8.

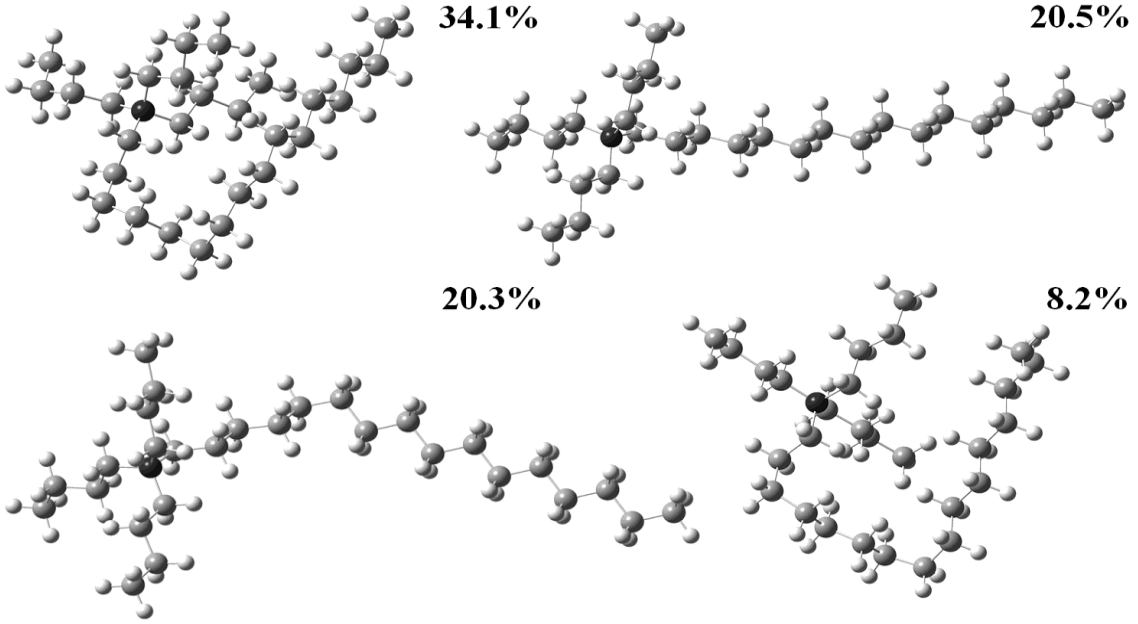

Fig. 8 Most stable conformers (83.1%) of BA cation. The numbers refer to the conformer weight in the thermal distribution. These are the results of a Monte Carlo conformational search using the MMFF94 force field

The results for the BP cation are presented in Fig. 9 where the 5 most stable conformers have 80.1% in the thermal distribution and it is needed 12 conformers to yield 95.1% of the total distribution.

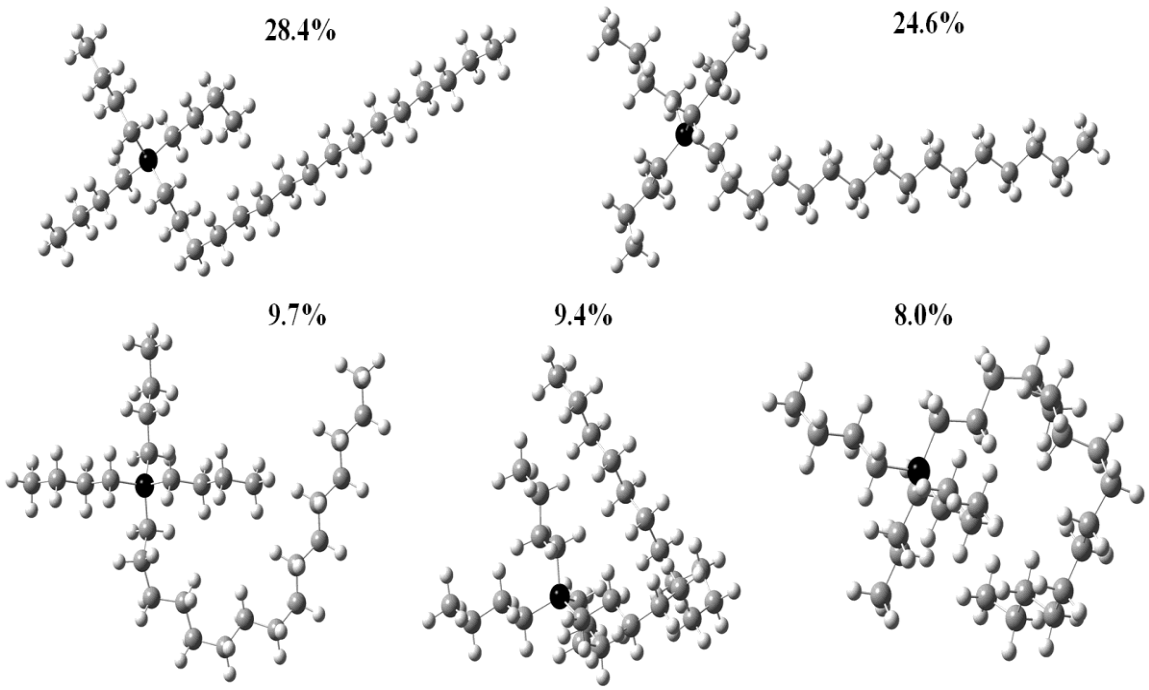

Fig. 9 Most stable conformers (80.1%) of BP cation. The numbers refer to the conformer weight in the thermal distribution. These are the results of a Monte Carlo conformational search using the MMFF94 force field

Comparing the results and illustrations presented in Figs. 7 to 9 it is clear that the size of the smaller alkyl chains has a profound impact into the conformation of the large alkyl chain, and this behavior is independent upon the heteroatom. For the trimethyl cations the conformation of the large alkyl chain is mostly extended (linear) *anti*, whereas for the tributyl cations the *gauche* or folded conformations have significant contributions. Also, for these latter cations the weights to the thermal distribution are spread over a larger number of conformers when compared to the trimethyl ones. It can also be visually assessed that this distinct behavior if probably due to the van der Waals interactions between the smaller alkyl chains, $CH_3(CH_2)_n$ (n = 0

and 3), of the ionic head and the large alkyl chain, where for n = 3 these interactions are favored and for n = 0 are not favored.
The quantitative values for the degree of folding of each conformer weighted by its Boltzmann factor calculated with MMFF94 (molecular mechanics) and AM1 (quantum chemical) methods are presented in Table 3.

Table 3 Calculated properties for the MA, BP, BA and MP cation conformers with MMFF94 and AM1 methods. Notation: "#" is the number of conformers needed to yield approximately 95% of the thermal distribution and "folding" is the degree of folding (%) calculated for each conformer and weighted for its Boltzmann factor

	MMFF94				AM1			
Cation	MA	MP	BA	BP	MA	MP	BA	BP
#	14	7	9	12	20	20	25	13
folding	22.5	15.5	53.5	37.4	37.7	29.5	51.6	45.4

These quantitative results allow for a more detailed comparison between the organic cations. From Table 3 it is statistically significant that the ammonium quaternary cations are more likely to yield folded conformations than the phosphonium ones. This trend is more evident for the cations with larger alkyl groups (tributyl) in the ionic head. These results are in qualitative agreement with the visual inspection of Figs. 7 to 9 and the Boltzmann weight of each conformer. In addition, this trend and other quantitative obtained with the MMFF94 method results are consistent with the results obtained with the AM1 method, but it should be kept in mind the intrinsic errors of ZDO (zero differential overlap) based methods (AM1, RM1, PM3, etc.) for performing conformational analysis and determining relative energies of conformers.

However, the main trend that tributyl groups in the ionic head induce folding of the large alkyl chain is clear in all analyses and suggests that the smaller PET intercalation in ANOBP organoclay is probably due to the fact that the BP cations are mostly folded, thus blocking the inclusion of the polymer within the clay galleries. Whereas the MA cation has a predominant linear or extended (*anti*) conformation, so that less hindrance for the polymer inclusion is caused by the surfactant. Also, the ionic head of MA cation is more exposed and less shielded by the alkyl groups, thus allowing it to interact more strongly with the polar groups of PET, in addition to an increase in the van der Waals interactions between the large alkyl chain in the extended conformation with the apolar chain of the polymer. The shielding of the Coulombic interactions of the ionic head by the tributyl groups can also be responsible for the observed smaller temperature for water loss. Also, the volumes of the folded conformations are larger than the extended ones, so that the former would cause a larger increase in the interlayer basal distances (d_{001}) compared to the latter ones. This reasoning explains results presented in Fig. 4, where BP induces larger interlayer separations than MA.

It should be noted that only to intercalation models have been proposed [7, 59], namely, paraffin and lateral, as depicted in Figs. 10a and 10b, respectively. However, our molecular modeling results suggest that a new model needs to be considered, namely, folded conformations arranged into a mono- or bi-layered systems, as illustrated in Fig. 10c.

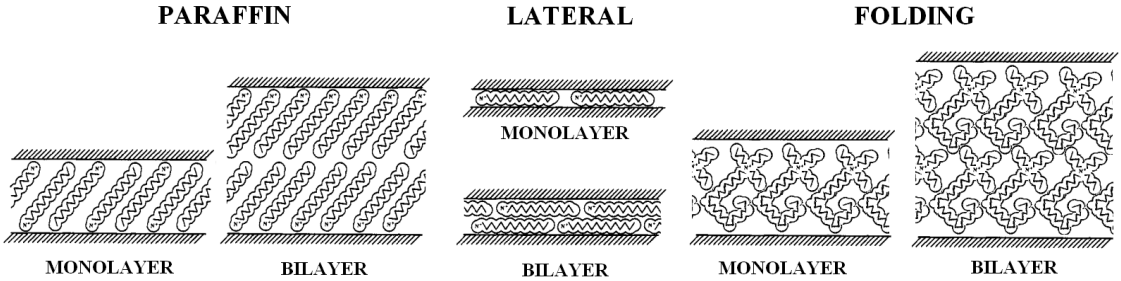

Fig. 10 Schematic representation of the intercalation models of surfactants within clay galleries. Models (a) and (b) are available in the literature and model (c) has been proposed based on the molecular modeling results

IV. CONCLUSION

Based upon the experimental results and the molecular modeling analyses we can conclude that the larger degree of folding of the C_{16} alkyl chain calculated for the BP, $(C_{16}H_{33}P(C_4H_9)_3)^+$, cation is responsible for promoting a larger increase in the modified clay galleries when compared to the MA, $(C_{16}H_{33}N(CH_3)_3)^+$, cation. Despite this larger basal separation in the organoclay ANOBP, it has smaller capacity for retaining polymer (PET) than ANOMA. This was explained by the hindrance caused by the cation folded conformation for polymer intercalation, as well as the smaller affinity (Coulombic shielding and decreased van der Waals

interactions) of these folded conformations towards the PET polar and apolar chains. These results and analyses suggested a new intercalation model for the BP and BA, $(C_{16}H_{33}N(C_4H_9)_3)^+$, surfactants where the folded conformations are significant. In addition, from the molecular modeling results it was predicted that the organoclay modified by BA cation would provide the least probable matrix for polymer intercalation and formation of nanocomposite with an intercalated morphology.

V. ACKNOWLEDGMENTS

The authors are grateful for the financial support from the CNPq (Brazilian Agency) and from RENAMI and INCT-INAMI (Brazilian Scientific Programs). Authors IFV and MVPS acknowledge CNPq for graduate scholarships.

VI. REFERENCES

[1] D Burgentzle, J Duchet, JF Gerard, A Jupin, B Fillon, *Journal Colloid Interface Science*, 278, 2004, 26.
[2] EP Giannelis, *Advanced Materials*, 8, 1996, 29.
[3] RA Vaia, EP Giannelis, *Macromolecules*, 30, 1997, 399.
[4] A Gu, SW Kuo, FC Chang, *Journal of Applied Polymer and Science*, 79, 2001, 1902.
[5] P Maiti, K Yamada, M Okamoto, K Ueda, K Okamoto, *Chemistry of Materials*, 14, 2002, 4654.
[6] E Manias, G Hadziioannou, G Brinke, *Langmuir*, 12, 1996, 4587.
[7] JH Wu, MM Lerner, *Chemistry of Materials*, 5, 1993, 835.
[8] HP He, RL Frost, T Bostrom, P Yuan, L Duong, D Yang, Y Xi, JT Kloprogge, *Applied Clay and Science*, 31, 2006, 262.
[9] MR Stackmeyer, *Applied Clay and Science*, 6, 1991, 39.
[10] LP Meier, R Nueesch, FT Madsen, *Journal Colloid and Interface Science*, 238, 2001, 24.
[11] LZ Zhu, B Chen, *Environmental Science and Technology*, 34, 2000, 2997.
[12] LZ Zhu, B Chen, XY Shen, *Environmental Science and Technology*, 34, 2000, 468.
[13] F Bergaya, G Lagaly, *Applied Clay Science*, 19, 2001, 1.
[14] G Lagaly, *Clay Mineralogy*, 16, 1981, 1.
[15] RA Vaia, RK Teukolsky, EP Giannelis, *Chemistry of Materials*, 6, 1994, 1017.
[16] YQ Li, H Ishida, *Langmuir* 19 (2003) 2479.
[17] HP He, RL Frost, JX Zhu, *Spectrochimica Acta*, Part A, 60, 2004, 2853.
[18] HP He, RL Frost, YF Xi, JX Zhu, *Journal Raman Spectroscopy*, 35, 2004, 316.
[19] YQ Li, H Ishida, *Chemistry of Materials*, 14, 2002, 1398.
[20] W Xie, ZM Gao, WP Pan, D Hunter, A Singh, RA Vaia, *Chemistry of Materials*, 13, 2001, 2979.
[21] W Xie, RC Xie, WP Pan, D Hunter, B Koene, LS Tan, RA Vaia, *Chemistry of Materials*, 14, 2002, 4837.
[22] S Yariv, *Applied Clay Science*, 24, 2004, 225.
[23] HP He, RL Frost, F Deng, JX Zhu, XY Weng, P Yuan, *Clays and Clay Minerals*, 52, 2004, 350.
[24] JX Zhu, HP He, LZ Zhu, XY Weng, F Deng, *Journal Colloid Interface Science*, 286, 2005, 239.
[25] SY Lee, SJ Kim, *Colloids and Surface*, 211, 2002, 19.
[26] SY Lee, SJ Kim, Clays and Clay Minerals, 50, 2002, 435.
[27] P Capková, M Pospíšil, J Miehé-Brendlé, M Trchová, Z Weiss, R Le Dred, *Journal Molecular and Modeling*, 6, 2000, 600.
[28] E Hackett, E Manias, EP Giannelis, *Journal Chemistry and Physics*, 108, 1998, 7410.
[29] G Tanaka, LA Goetter, *Polymer*, 43, 2002, 5915.
[30] AC Balazs, C Singh, E Zhulina, *Macromolecules*, 31, 1998, 8370.
[31] GW Phelps, DL Harris, *Americam Ceramics Society Bulletin*, 47, 1968, 1146.
[32] IF Leite, APS Soares, LH Carvalho, CMO Raposo, OML Malta, SML Silva, *Journal of Thermal Analysis and Calorimetry*, 100, 2009, 563.
[33] SML Silva, PER Araújo, KM Ferreira, EL Canedo, LH Carvalho, CMO Raposo, *Polymer Engineering and Science*, 49, 2009, 1696.
[34] MJS Dewar, E Zoebisch, E Healy, JJP Stewart, *Journal American Chemistry Society*, 107, 1985, 3902.
[35] MJS Dewar, C Jie, *Journal Molecular and Structure*, (THEOCHEM), 187, 1989, 1.
[36] TA Halgren, *Journal of Computer Chemistry*, 17, 1996, 490.
[37] DC Rodríguez-Sarmiento, JA Pinzón-Bello, *Applied Clay Science*, 18, 2001, 173.
[38] J Madejová, *Vibrational Spectroscopy*, 31, 2003, 1.
[39] M Kozak, L Domka, *Journal Physics and Chemistry Solids*, 65, 2004, 441.
[40] Y Xi, Z Ding, H He, RL Frost, *Spectrochimica Acta A*, 61, 2005, 515.
[41] M Madjan, O Maryuk, A Plaska, S Pikus, R Kwiatkowski, *Journal Molecular and Structure*, 874, 2008, 101.
[42] HP He, FL Ray, Z Jianxi, *Spectrochimica Acta*, *Part A*, 60, 2004, 2853.

[43] NV Venkataraman, S Vasudevan, *Journal of Physical and Chemistry B*, 105, 2001, 1805.
[44] M Bora, JN Ganguli, DK Dutta, *Thermochimica Acta*, 346, 2000, 169.
[45] WH Awad, JW Gilman, M Nyden, RH Harris, TE Sutto, J Callahan, PC Trulove, HC Delong, DM Fox, *Thermochimica Acta*, 409, 2004, 3.
[46] S Mendioroz, JA Pajares, J Benito, C Pesquera, F Gonzáles, C Blanco, *Langmuir*, 3, 1987, 676.
[47] J Madejová, M Janek, P Komadel, HJ Herbert, HC Moog, *Applied Clay Science*, 20, 2002, 255.
[48] X Kornmann, *Polymer*, 42, 2001, 1303.
[49] T Yui, H Yoshida, H Tachibana, DA Tryk, H Inoue, *Langmuir*, 18, 2002, 891.
[50] Z Klapyta, T Fujita, N Iyi, *Applied Clay Science*, 19, 2001, 5.
[51] HA Patel, RS Somani, H. Bajaj, RV Jasra, *Applied Clay Science*, 35, 2007, 194.
[53] CB Hedley, G Yuan, BKG Theng, *Applied Clay Science*, 35, 2007, 180.
[54] A Leszczynska, J Njuguna, K Pielichowski, JR Banerjee, *Thermochimica Acta*, 453, 2007, 75.
[55] W Xie, Z Gao, K Liu, W Pan, R Vaia, D Hunter, A Singh, *Thermochimica Acta*, 367-368, 2001, 339.
[56] M Kawasumi, N Hasegawa, M Kato, A Usuki, A Okada, *Macromolecules*, 30, 1997, 6333.
[57] J Cho, DR Paul, *Polymer*, 42, 2001, 1083.
[58] A Sánchez-Solís, A Garcia-Rejon, O Manero, *Macromolecular Symposia*, 192, 2003, 281.
[59] SS Ray, M Okamoto, *Progress Polymer Science*, 28, 2003, 1539.